Oxidative Stress is Intrinsic to Staphylococcal Adaptation to Fatty Acid Synthesis Antibiotics

Paprapach Wongdontree [1], Aaron Millan-Oropeza [2], Jennifer Upfold [1], Jean-Pierre Lavergne [3], David Halpern [1], Clara Lambert [4], Adeline Page [5], Gérald Kénanian [1], Christophe Grangeasse [3], Céline Henry [2], Agnès Fouet [4], Karine Gloux [1], Jamila Anba-Mondoloni [1], Alexandra Gruss [1*]

[1] Université Paris-Saclay, INRAE, AgroParisTech, Micalis Institute, 78350, Jouy-en-Josas, France. [2] PAPPSO Platform, Université Paris-Saclay, INRAE, AgroParisTech, Micalis Institute, Jouy-en-Josas, France. [3] Bacterial Pathogens and Protein Phosphorylation, Molecular Microbiology and Structural Biology, UMR 5086 - CNRS / Université de Lyon, Building IBCP, 7 Passage du Vercors, Lyon, France. [4] Université Paris Cité, Institut Cochin, INSERM, U1016, CNRS, UMR8104, Paris, France. [5] Protein Science Facility, SFR BioSciences, CNRS, UMS3444, INSERM US8, Université de Lyon, Lyon, France

* For correspondence: alexandra.gruss@inrae.fr

Key words: Fatty acid synthesis (FASII) pathway/antibiotic adaptation/peroxide priming/fitness/ virulence.

Short title: FASII bypass redirects *S. aureus* fitness

Abstract

Antibiotics inhibiting the fatty acid synthesis (FASII) pathway of the major pathogen *Staphylococcus aureus* reach their enzyme targets, but bacteria continue growth by using environmental fatty acids (eFAs) to produce phospholipids. We assessed how extreme changes in membrane phospholipids provoked by FASII-antibiotics affect global *S. aureus* physiology. Anti-FASII provoked massive lasting expression changes without genomic rearrangements. Several regulators, rather than one master switch, contributed to the timing of anti-FASII adaptation. Numerous virulence and adhesion factors showed decreased levels and/or activity. Conversely, stress response protein levels increased, and correlated with greater tolerance to peroxides. Notably, peroxide priming stimulated eFA incorporation efficiency and facilitated adaptation to FASII inhibition. These findings establish a link between oxidative stress and FA incorporation. Consistent with major shift in protein expression, anti-FASII-adapted *S. aureus* killed an insect host more slowly but continued multiplying. Thus, while anti-FASII-adapted populations are less equipped to damage the host, they may be better fit for long term survival, and could constitute a reservoir for re-infection.

41 **Introduction**

42 *Staphylococcus aureus* is a Gram-positive opportunistic bacterium that remains a major cause
43 of disease and mortality in humans and animals. The unsolved crisis of non-treatable infections
44 due to multidrug-resistance notably methicillin-resistant *S. aureus* (MRSA) underlines the need
45 for alternative treatments, especially in compromised patients (Lowy, 1998, Rasigade and
46 Vandenesch, 2014, Lakhundi and Zhang, 2018, Cusumano et al., 2020).

47 Enzymes of the fatty acid (FA) synthesis pathway (FASII) are longtime candidate targets for
48 drug development against *S. aureus* infections (Wang et al., 2006, Wright and Reynolds, 2007).
49 FabI, enoyl-ACP reductase, was a preferred target as a narrow spectrum inhibitor that would
50 not disrupt the gut microbiome during treatment (Karlowsky et al., 2009). However, while anti-
51 FASII drugs targeting FabI effectively reached their targets in *S. aureus*, bacterial growth
52 continued in *in vitro* or mouse bacteremia models; this is because bacteria incorporate
53 environmental FAs (eFAs), which are abundant in host biotopes and are used directly to
54 produce bacterial membrane phospholipids; the process is termed FASII bypass (Brinster et al.,
55 2009, Gloux et al., 2017, Kenanian et al., 2019, Morvan et al., 2016) (**Fig. S1** schematizes FASII
56 and FASII bypass pathways). Exposure to host lipids during septicemic infection thus favors *S.*
57 *aureus* adaptation to anti-FASII treatment (Kenanian et al., 2019). Despite these limitations of
58 FASII antibiotics in treating streptococcal, enterococcal, and staphylococcal infections, new
59 anti-FASII drugs are in development (Pishchany et al., 2018, Yao and Rock, 2016, Fage et al.,
60 2020, Parker et al., 2022). Characterizing the anti-FASII-adapted *S. aureus* populations that
61 might persist in the host after treatment is thus crucial for future use.

62 We report here that anti-FASII treatment results in the emergence of a novel *S. aureus*
63 fitness state. Anti-FASII-adapted bacteria produce less virulence factors. In contrast, stress
64 responses are activated, and adapted bacteria show greater peroxide tolerance. Pre-exposure
65 to peroxides accelerates anti-FASII adaptation by enhancing fatty acid incorporation, thus
66 identifying a new strategy by which peroxide priming facilitates antibiotic survival. These

67 findings elucidate the state of anti-FASII-adapted bacteria that persist in the host after anti-
68 FASII treatment.

69 **Results**

70 **Anti-FASII treatment leads to long-term *S. aureus* adaptation without detectable**
71 **chromosomal rearrangements.** Our previous studies ruled out a role for point mutations or
72 indels in *S. aureus* adaptation to anti-FASII in serum-containing medium; studies were
73 performed using either of two potent FabI inhibitors, triclosan (McMurry et al., 1998) or AFN-
74 1252, a pipeline antimicrobial with high FabI specificity (Karlowsky et al., 2009), giving equivalent
75 results (Kenanian et al., 2019). As large chromosomal rearrangements are not detected by mi-
76 Seq (Kenanian et al., 2019), we resorted to nanopore sequencing of four anti-FASII-adapted
77 cultures. Tests were performed using AFN-1252 and two non-treated cultures. No
78 rearrangements specific to anti-FASII adaptation were detected, showing that anti-FASII-
79 adaptation occurs in the absence of chromosomal rearrangements or mutations. Once adapted
80 to anti-FASII, growth was robust in SerFA liquid medium (BHI supplemented with serum and
81 fatty acids); however, bacteria grew poorly in FA-free medium (**Fig. S2**). These results indicated
82 that phenotypic alterations were responsible for anti-FASII adaptation.

83 **Anti-FASII adaptation involves massive protein reprogramming.** A proteomics approach was
84 used to elucidate changes occurring during anti-FASII adaptation. FASII inhibition is overcome
85 by eFAs provided in the presence of serum. Serum protects bacteria from toxic free FAs, and
86 promotes FASII bypass (Kenanian et al., 2019). A complete kinetics study on *S. aureus* USA300
87 used the anti-FASII triclosan, both without and with added serum, at 2, 4, 6, 8, and 10 h post-
88 anti-FASII addition (**Fig. 1A, B, C** respectively show strategy, growth kinetics, and proteome
89 results; **Table S1, tabs 1 and 2,** give complete results according to cluster analyses). As
90 expected, protein abundance was mainly lower in triclosan medium (FA-Tric) without serum,
91 where adaptation occurs by mutation emergence (Morvan et al., 2016). In contrast, massive
92 protein level changes in adaptation (SerFA-Tric) medium suggest metabolic activity in latency

93 phase prior to full outgrowth, with transient or lasting expression differences compared to non-
94 treated bacteria (compare SerFA and SerFA-Tric, **Fig. 1C**).

95 We first exploited the data to screen for proteins whose levels selectively increased in the
96 presence of specific signals related to FAs and/or anti-FASII (**Fig. S3**). Highest expression of
97 several Type 7 secretion system proteins (comprised between SAUSA300_0278 and
98 SAUSA300_0289) occurred in FA conditions, as reported (Lopez et al., 2017). The FarE fatty acid
99 efflux pump was also up-regulated, presumably to avoid accumulation and toxicity of free FAs
100 (Alnaseri et al., 2015); as reported, induction was alleviated in serum, which lowers toxicity
101 (Kenanian et al., 2019). Overall, serum markedly affects *S. aureus* responses to anti-FASII, thus
102 highlighting its crucial role in adaptation.

103 Proteins related to FASII and phospholipid metabolism showed striking differences
104 according to conditions (**Fig. S4**). Levels of most FASII- and phospholipid-related enzymes
105 increased in SerFA-Tric as compared to those in all other conditions, including FA-Tric without
106 serum. Notably, PlsC (1-acyl-sn-glycerol-3-phosphate acyltransferase), is required for
107 phospholipid synthesis and anti-FASII adaptation. After an initial decrease, PlsC levels are then
108 restored during adaptation outgrowth, in accordance with results using a reporter fusion
109 (Pathania et al., 2021). This result highlights the importance of serum in enabling FASII bypass.

110 We focus below on the changes occurring in serum-supplemented medium containing anti-
111 FASII (SerFA), in which FASII bypass occurs without genetic modification. Three categories of
112 proteins, regulators, stress response proteins, and virulence factors, are analyzed.

113 **Anti-FASII adaptation triggers shifts in regulatory protein expression and phosphorylation.**
114 Regulatory proteins are likely implicated in the massive changes caused by anti-FASII
115 treatment. Proteomics revealed 22 hypothetical or confirmed proteins implicated in regulation
116 whose expression decreased (9) or increased (13) during anti-FASII adaptation; they affect
117 stress response, virulence, nutritional immunity and metabolism, or combinations of these
118 factors (**Fig. 2A**). As phosphorylation is a frequent post-translational modification that alters

119 functions of numerous regulatory proteins (Garcia-Garcia et al., 2016, Mijakovic et al., 2016,
120 Derouiche et al., 2013), we performed a phosphoproteomics analysis, focusing here on
121 regulatory proteins. Five regulators showed altered phosphorylation patterns during transition
122 or upon adaptation to anti-FASII (**Fig. 2B** and **Fig. S5**; **Table S2** for full results). Altogether, we
123 selected CcpE, CshA, HrcA, Rot, and XdrA as showing high expression and/or phosphorylation
124 changes at or just prior to adaptation outgrowth (8-10 h) (**Fig. 2A and B**) for further study**.**

125 To determine how these regulators affected anti-FASII adaptation, we compared growth
126 kinetics of USA300 and the corresponding mutant strains (Fey et al., 2013) (**Fig. 2C**). The
127 absence of *cshA* led to ~2 h delays in anti-FASII adaptation time. CshA controls the supply of
128 acetyl-CoA; its interruption results in phospholipids enriched in saturated FAs (Khemici et al.,
129 2020). We propose that this membrane alteration might interfere with eFA incorporation.

130 The *xdrA* mutant also showed a 2 h delay in adaptation. Both the amounts and
131 phosphorylation of XdrA decreased during anti-FASII treatment. The putative fatty acid
132 degradation gene *fadX* is reportedly upregulated when XdrA pools are lower (McCallum et al.,
133 2010), which might transiently compete for eFAs and limit their availability for FASII bypass.
134 Alternatively, XdrA DNA binding activity reportedly overlaps that of the CodY regulator (Lei and
135 Lee, 2018). We recently showed that a *codY* mutant is delayed in adaptation, which we
136 proposed relates to a positive regulatory effect of CodY on Acc expression (Pathania et al.,
137 2021). The delay in anti-FASII adaptation of the *xdrA* mutant might relate to a coordinate role
138 between XdrA and CodY. *hrcA* and *ccpE* mutants showed minor changes in anti-FASII
139 adaptation kinetics, while *rot* had no detectable change (**Fig. 2C**).

140 Thus, while regulatory mutants individually affect anti-FASII-adaptation efficacy, no single
141 tested regulator acted as a master controller. In *Escherichia coli*, stress response regulators
142 respond to discrete extracytoplasmic signals, each of which independently contributes to stress
143 adaptation (Bury-Mone et al., 2009). Similarly, differentially expressed regulators may each

144 respond to different stimuli consequent to membrane perturbation by anti-FASII, which
145 cooperatively promote adaptation.

146 **Reduced levels and activities of virulence factors in anti-FASII-adapted *S. aureus*.** Levels of 10
147 out of 16 detected virulence-related proteins decreased transiently or durably during anti-FASII
148 adaptation compared to non-treated *S. aureus* cultures (**Fig. 3A**). Levels of several adhesins
149 were markedly decreased, including ClfB, which is required for virulence (Dyzenhaus et al.,
150 2022); iron receptor protein and toxin levels were also overall reduced. In contrast, two
151 peptidoglycan hydrolases, Atl and IsaA, showed increased levels. Hydrolases are implicated in
152 housekeeping, and also in virulence (Stapleton et al., 2007); their increased expression upon
153 adaptation outgrowth might resolve cell wall thickening in the latency phase (PW, AG, JAM, in
154 preparation). We asked whether decreased amounts of adhesion factors SdrD, SdrE, EbpS, and
155 ClfB in anti-FASII-adapted *S. aureus* might impact adhesion to host cells. Anti-FASII-adapted *S.*
156 *aureus* (using AFN-1252) adhered poorly to human THP-1 macrophages compared to non-
157 adapted bacteria (20% *versus* 44%, $p < 0.01$; **Fig. 3B**). We also evaluated major secreted
158 virulence factors not detected by proteomics: lipase, nuclease, protease, and hemolysin in non-
159 treated *versus* anti-FASII-adapted *S. aureus* cultures (**Fig. 3C**). Activities of these exoproteins
160 were visibly lower in anti-FASII adapted cultures obtained using triclosan or AFN-1252.
161 Altogether these results indicated that anti-FASII-adapted *S. aureus* populations may be less fit
162 for virulence.

163

164 **Anti-FASII-adapted *S. aureus* produce increased levels of stress response proteins and show**
165 **increased resistance to an oxidative stress.** Levels of 26 out of 28 assessed stress response
166 proteins showed transient or lasting increases in anti-FASII-adapted *S. aureus* compared to the
167 non-treated control. Among them, 18 were pronounced in during adaptation outgrowth.
168 Proteins are implicated in pH, oxidative, osmotic, and unfolded protein responses (**Fig. 4A**).

169 Host production of reactive oxidative species (ROS) is a documented response to infection
170 as a means to eliminate the pathogen (Liu et al., 2005). We asked whether increased levels of

171 stress-related factors in anti-FASII-adapted *S. aureus* affected bacterial tolerance to ROS. This
172 was tested by challenging non-treated and anti-FASII-adapted cultures with 0.5 mM H_2O_2 for 5
173 h, followed by survival assessments by colony forming unit (CFU) determinations. Anti-FASII-
174 adapted *S. aureus* CFUs were ~20-fold higher than for non-treated bacteria ($p < 0.01$; **Fig. 4B**).
175 Greater peroxide tolerance might thus confer a survival advantage to the anti-FASII-adapted,
176 oxidative stress-resistant populations.

177 **Priming with peroxides prior to anti-FASII challenge stimulates adaptation by enhancing eFA**
178 **incorporation, and requires PerR.** Stress response induction by anti-FASII led us to ask the
179 contrary, whether stress priming would stimulate anti-FASII bypass. A ROS priming effect
180 reportedly increased resistance to various antibiotics in *E. coli*, including oxolinic acid,
181 ampicillin, kanamycin (Mosel et al., 2013), and fluoroquinolones (Gerstel et al., 2020). The
182 effects of ROS priming on anti-FASII adaptation in *S. aureus* were tested by subjecting cultures
183 to overnight priming with sub-lethal concentrations of H_2O_2 (0.5 mM) or phenazine-
184 methosulfate (PMS, a redox cycling compound; 20-50 µM (Gerstel et al., 2020)). Cultures were
185 diluted, and kinetics of anti-FASII (AFN-1252) adaptation was followed. H_2O_2 or PMS priming
186 shortened the time of *S. aureus* adaptation to FASII antibiotics by 1.5 – 1.7 h compared to non-
187 primed WT cultures (**Fig. 4C upper**, **Table 1**). A *katA* mutant lacks catalase and would
188 accumulate H_2O_2; anti-FASII adaptation in *katA* was ~1 h shorter than in the WT parental strain.
189 Priming *katA* with H_2O_2 as above further shortened the adaptation time by ~2 h as compared
190 to WT without peroxide (**Table 1**). Conversely, treating the WT strain with reducing agents (Na
191 citrate 10 mM, or vitamin C 5.7 mM) retarded adaptation by 3.5 and 1.7 h respectively (**Table**
192 **1**). *S. aureus* oxidation state is thus implicated in anti-FASII adaptation.

193 ROS priming induces antibiotic efflux in *E. coli*, leading to antibiotic tolerance (Gerstel et al.,
194 2020, Mosel et al., 2013, Wu et al., 2012). Induction of the *E. coli* Fe-S repair system Suf matures
195 the SoxR regulator, which in turn activates the AcrAB efflux pump to eliminate
196 fluoroquinolones (Gerstel et al., 2020). We asked whether peroxide similarly induces an efflux

197 mechanism that would accelerate anti-FASII adaptation. If this were the case, FASII activity
198 would be restored, and bacteria would be anti-FASII-sensitive. However, examination of FA
199 profiles revealed the contrary: at 6 h post anti-FASII treatment (using AFN-1252), *i.e.*, during
200 the latency phase, H_2O_2 priming resulted in more efficient eFA incorporation compared to that
201 in non-primed cultures (respectively 82% *versus* 54% eFAs; **Fig. 4C**). Moreover, a transposon
202 insertion inactivating the *suf* homolog in *S. aureus* (Roberts et al., 2017) did not abolish the
203 H_2O_2 priming effect (**Table 1**). These results show that stimulated eFA incorporation and hence
204 more rapid adaptation, rather than anti-FASII efflux, explains the priming effects of peroxide
205 on anti-FASII adaptation.

206 PerR (SAUSA300_1842) is a conserved highly sensitive metal-dependent peroxide sensor
207 and regulator protein (Ji et al., 2015). PerR was not detected in proteomics of anti-FASII
208 adaptation (**Table S1**). However, as PerR senses H_2O_2, we examined its implication in H_2O_2-
209 accelerated anti-FASII adaptation. Unlike the USA300 parent, *perR* mutant adaptation time and
210 FA incorporation efficiency were unaffected by peroxide (proportions of eFA incorporation at
211 6 h were 52% and 51%, with and without H_2O_2 priming; **Fig. 4C**). Altogether these results
212 indicate the existence of a unique H_2O_2 priming system that requires PerR. They reveal a novel
213 link between peroxide and FA incorporation that facilitates adaptation to the FASII class of
214 antibiotics independently of antibiotic efflux.

215 **Anti-FASII-adapted *S. aureus* are less virulent, yet persist in a *Galleria mellonella* infection**
216 **model.** Lower virulence factor production but greater stress resistance due to anti-FASII
217 adaptation raises questions on the outcome of anti-FASII-adapted *S. aureus* infection. We
218 compared anti-FASII-adapted *versus* non-treated *S. aureus* in an insect *G. mellonella* model,
219 which allows the use of a large cohort. Moreover, larval hemocoel, like blood serum, is lipid-
220 rich (Kazek et al., 2021). AFN-1252, as chosen for this study, was pharmacologically vetted for
221 non-toxicity in the host (Hunt et al., 2016, Parsons et al., 2011); we showed previously that
222 AFN-1252 treatment did not stop infection in a mouse model (Kenanian et al., 2019). Non-

223 treated and AFN-1252-adapted *S. aureus* USA300 showed equivalent growth kinetics in SerFA
224 *in vitro* (**Fig. S2**). Insects infected by 10^6 anti-FASII-adapted bacteria were killed more slowly
225 than those infected by equivalent CFUs of untreated bacteria, as monitored over 72 h post-
226 infection (**Fig. 5A**). At T_{48}, 95% of insects were killed by untreated *S. aureus*, compared to 30%
227 killing with anti-FASII-adapted *S. aureus*. At T_{72}, when all larvae infected by untreated *S. aureus*
228 were dead, anti-FASII-adapted *S. aureus* killed over 60% of the insects. Thus, killing by anti-
229 FASII-adapted *S. aureus* was delayed but not stopped.

230 Bacterial CFUs determined from infected insects at 24 h were about 3-fold lower in those
231 infected by anti-FASII-adapted compared to non-treated bacteria, and then decreased in
232 surviving insects (**Fig. 5B left**). In contrast, CFUs in dead larvae at T_{48} were comparable for both
233 groups, indicating that anti-FASII-adapted bacteria multiplied as well as non-treated bacteria
234 in the insects they killed (**Fig. 5B right**).

235 To determine whether anti-FASII-adapted bacteria remained adapted during infection, CFU
236 platings as above were done in parallel on SerFA and SerFA-AFN solid media. Only anti-FASII-
237 adapted bacteria formed colonies on SerFA-AFN solid medium (**Table S3**). Among surviving
238 insects infected with adapted bacteria, only one contained bacteria that returned to the non-
239 adapted state at 72 h; this indicates that bacteria remained mainly adapted during insect
240 infection. Altogether, these results show that anti-FASII-adapted *S. aureus* are less virulent,
241 while populations still multiply in the insect host. Greater stress resistance capacity may help
242 withstand host conditions and can explain bacterial persistence in the insect host.

243

244 **Discussion**

245 eFA incorporation during FASII-antibiotic-induced bypass redesigns *S. aureus* membrane
246 phospholipids, leading to massive shifts in protein expression, and a prolonged adaptation
247 state without detectable genomic rearrangements or mutations (summarized in **Fig. 6** model).
248 These changes, which begin before bacterial outgrowth, alter the *S. aureus* fitness state

249 towards less damage to the host, and more tolerance to host-generated toxicity. Peroxide
250 priming accelerates adaptation and eFA incorporation, establishing a link between ROS and
251 FASII bypass. The *in vitro* phenotypes deduced from proteomic and *in vitro* findings are
252 consistent with the differences observed in insect infection kinetics between non-treated and
253 anti-FASII-treated *S. aureus*.

254 **Regulator changes during anti-FASII treatment.** Various regulators appear to be implicated in
255 anti-FASII adaptation, *e.g.*, XdrA or CshA, and to lesser extents HrcA or CcpE. However, no single
256 regulator was found to have a "master" role. In addition to alterations in protein abundance
257 and phosphorylation levels as assessed here, we hypothesize that membrane perturbations, as
258 caused by anti-FASII, alter the intracellular environment, to liberate signaling lipids that
259 modulate regulator activities (**Fig. 6**). For example, FAs and cardiolipin reportedly affect
260 activities of the *S. aureus* two-component system SaeRS (Schurig-Briccio et al., 2020, Yeo et al.,
261 2023). Virulence factor activity may be blocked by FA binding as shown in *Vibrio cholerae*
262 (Lowden et al., 2010). Interaction of regulators with lipid species released during anti-FASII
263 treatment may be a rapid means to adjust regulator functions for FASII bypass.

264 **Link between FASII-antibiotic adaptation and *S. aureus* fitness against peroxide stress.** We
265 showed that ROS priming stimulates FASII bypass by increasing eFA incorporation (**Fig. 4**). To
266 our knowledge, this is the first report establishing a connection between oxidative stress and
267 stimulation of FASII antibiotic adaptation, and defines a novel paradigm. This mechanism
268 contrasts to that described in *E. coli*, where ROS priming either lowered proton-motive-force-
269 mediated antibiotic entry and/or induced efflux pump expression, *via* a Suf-controlled Fe-S
270 repair system (Gerstel et al., 2020). In contrast, the H_2O_2-stimulated anti-FASII adaptation is
271 mediated by greater, rather than less, eFA incorporation and precocious adaptation, ruling out
272 a role for efflux. A *suf* mutant remained sensitive to peroxide activation, further distinguishing
273 the two mechanisms.

274 We hypothesize that H_2O_2 has a direct role in stimulating FASII bypass: H_2O_2–mediated
275 oxidation of FASII initiation enzymes could diminish competition with the FASII bypass system
276 (**Fig. 6**). We show here that a *katA* mutant, which presumably accumulates H_2O_2, shortens
277 adaptation time, while a *perR* mutant, which activates KatA to degrade H_2O_2, lengthens
278 adaptation time. Direct or indirect targets of H_2O_2 could be involved in disabling FASII to favor
279 FASII bypass; this hypothesis is currently under study.

280 Host macrophages and neutrophils generate peroxides presumably as a means to control
281 infection (Cole et al., 2014, Mayer-Scholl et al., 2004). *S. aureus* adaptation to anti-FASII is
282 potentiated in these same conditions, which needs to be considered for future use of FASII
283 antibiotics.

284 **Potential advantages of a fitness reset in FASII-antibiotic-adapted *S. aureus*.** Lower virulence,
285 greater stress response, and exclusive eFA utilization may be advantageous to *S. aureus*
286 lifestyle. We note that streptococci and enterococci use FASII bypass even without antibiotics,
287 favoring eFA incorporation during infection (Brinster et al., 2009, Lambert et al., 2023).
288 Although these species employ distinct FASII regulation system from that of *S. aureus* (feedback
289 *versus* feedforward in *S. aureus* (Lambert et al., 2022, Albanesi et al., 2013)) and differ in their
290 *in vivo* lifestyles, they have common infection biotopes, raising the possibility that FASII bypass
291 is advantageous in the course of infection.

292 Parallels also exist between anti-FASII-adapted *S. aureus*, and small colony variants (SCVs):
293 both emerge more efficiently in oxidative stress (Peyrusson et al., 2022, Painter et al., 2015),
294 and both produce less virulence factors (Tuchscherr et al., 2020, Sendi and Proctor, 2009),
295 which might facilitate bacterial escape from host immune surveillance. In both cases,
296 uneradicated reservoirs of these bacteria might be sources of chronic infection (**Fig. 6**).

297 **Potential applications of FASII antibiotics.** Although anti-FASII do not eliminate *S. aureus* when
298 compensatory eFAs are available, the present study demonstrates that it reduces *S. aureus*
299 virulence factor production. Anti-FASII synergy with other treatments that prevent adaptation

300 may potentiate its efficacy (Pathania et al., 2021). Here, anti-oxidants delayed anti-FASII
301 adaptation, which may offer perspectives for a bi-therapy approach to eliminate *S. aureus* with
302 reduced virulence.
303
304 **Materials and Methods**
305 **Strains, media, and growth conditions.** Experiments were performed using *S. aureus*
306 SAUSA300_FPR3757 JE2 strain, referred to as USA300, and transposon insertion derivative
307 strains from the Nebraska mutant library ((Fey et al., 2013); generously supplied by BEI
308 Resources NIAID, NIH, USA). All strains were confirmed for transposon insertion by PCR (see
309 **Table S4** for strains and primers used**)**. Cultures were grown aerobically at 37°C. Solid and liquid
310 growth media were based on BHI as follows: no additives (BHI), containing 0.5 mM FAs (BHI-
311 FA, with an equimolar mixture of 0.17 mM each C14, C16, C18:1 [Larodan, Sweden]), and BHI-
312 FA containing 10% newborn calf serum (Ser-FA; Eurobio Scientific, France [Fr]). Where
313 specified, the anti-FASII triclosan (McMurry et al., 1998) was added at 0.25 µg/ml in media
314 without serum, and at 0.5 µg/ml in media containing serum, to respectively give BHI-Tric, FA-
315 Tric, or SerFA-Tric, as described (Morvan et al., 2017, Kenanian et al., 2019, Morvan et al.,
316 2016). H_2O_2 (0.5 mM final concentration) was added to SerFA precultures when indicated. The
317 anti-FASII AFN-1252 (Karlowsky et al., 2009) was used in SerFA at 0.5 µg/ml (SerFA-AFN) as
318 described (Kenanian et al., 2019). For most experiments, *S. aureus* USA300 was streaked on
319 solid BHI medium, and independent colonies were used to inoculate overnight BHI pre-
320 cultures. For proteomic and phosphoproteomic studies, cultures were inoculated at a starting
321 OD_{600} = 0.1.
322 **Nanopore sequencing.** Six single colonies of USA00 were resuspended in SerFA and grown
323 overnight. Cultures were then diluted in SerFA, SerFA-AFN-1252, 10% mouse serum, or 10%
324 mouse serum containing AFN-1252, and grown to OD_{600} = 1. Whole chromosomal DNA was
325 prepared from the independent cultures as described, and outsourced for nanopore

326 sequencing (Eurofins, Germany). Whole genome DNA sequences were presented as
327 circularized genomes, and entered in the Mendeley database doi:10.17632/grt4htck9k.1.
328 Sequences were compared by performing full genome alignments
329 https://dgenies.toulouse.inra.fr/ 09/02/2023.

330 **Proteomics preparation.** Adaptation to anti-FASII varies with growth media: BHI-Tric-grown
331 and FA-Tric-grown *S. aureus* do not adapt in the time periods tested, (high frequency adaptive
332 mutations arise with a delay in FA-Tric; (Morvan et al., 2016)), whereas SerFA-Tric-grown *S.*
333 *aureus* adapt without mutation after an initial latency period (6-8 hours, depending on growth
334 conditions) (Kenanian et al., 2019). Kinetics experiments were performed on USA300 to
335 determine the protein changes associated with FA-Tric and SerFA-Tric anti-FASII adaptation.
336 Cultures for each condition were prepared as independent quadruplicates. For each sample,
337 BHI precultures were diluted and shifted to the specified medium starting cultures at OD_{600} =
338 0.1. Control cultures in BHI, BHI-FA and BHI-SerFA were grown to OD_{600} = ~1. BHI-Tric cultures
339 (no added FAs) were collected at 6 h. USA300 samples grown in FA-Tric and SerFA-Tric were
340 collected at 2, 4, 6, 8 and 10 h post-antibiotic addition (see **Fig. 1A** and **Table S1** for growth
341 conditions and complete data). For each sample, 20 OD_{600} units culture equivalent was
342 collected and centrifuged for 10 min at 4°C at 8000 rpm. Pellets were washed twice in Tris
343 10mM pH7.0 containing 0.02% TritonX-100, and Halt™ Protease & Phosphatase Inhibitor
344 Cocktail (100X) (Thermo Scientific, Fr). Pellets were then resuspended in 650 µl washing buffer,
345 mixed with 0.1 mm silica beads and subjected to 3 cycles of vigorous shaking (Fast-Prep-24,
346 MP-Bio, Fr). After 10 min centrifugation at 10000 rpm, supernatants were recovered and stored
347 at -80°C prior to analyses.

348 Protein extractions, LC-MS/MS analyses, and bioinformatics, and statistical data analyses
349 were done as described in detail (Bednarz et al., 2021). The reference genome GenBank
350 Nucleotide accession code NC_007793.1 was used for protein annotation. The bioinformatic
351 tools used for proteomics analysis (X!TandemPipeline C++, MassChroQ, MCQR) are open and

352 free resources available in the following repository: https://forgemia.inrae.fr/pappso. The
353 mass spectrometry proteomics data was deposited to the ProteomeXchange Consortium
354 (http://proteomecentral.proteomexchange.org) via the PRIDE partner repository with the
355 dataset identifier PPXD034256.

356 **Proteome data analyses.** Protein abundance differences were detected by ANOVA tests for all
357 methods used (spectral counting, SC; extracted ion chromatograms, XIC; and peak counting,
358 PC). The abundance of a protein was considered significantly variable when the adjusted p-
359 value was <0.05. Proteins showing significant statistical abundance differences were
360 represented on heat maps normalized by using GraphPad Prism 9.5.1 (Bednarz et al., 2021). K-
361 means clustering analysis was performed using RStudio. Proteins whose abundancies were
362 significantly different in one or more conditions were manually curated and classified according
363 to functional groups.

364 **Phosphoproteome preparation.** USA300 cultures were prepared in BHI and SerFA and
365 harvested at OD_{600} = ~1. SerFA-Tric cultures were harvested at 6h and 10 h post-treatment.
366 Samples were prepared independently from those in the proteomics study, as independent
367 biological triplicates, and treated as in proteomics studies, except that we collected the
368 equivalent of 50 OD_{600} units. Bacteria were processed as for proteome extraction except that
369 Tris was replaced by triethylammonium bicarbonate (50 mM; *n.b.* Tris interferes with dimethyl
370 tag labelling) containing antiprotease and antiphosphatase at the recommended
371 concentrations. Lysed bacteria after Fast-Prep were centrifuged 15 min at 12000 rpm
372 supernatants containing soluble proteins were kept at -80°C before use. Protein concentrations
373 were determined by the Bradford method.

374 One mg protein samples were evaporated and resuspended in 1 ml 5 % formic acid and
375 dimethyl-tag labeled as described (Boersema et al., 2009). Briefly, differential on-column
376 labeling of peptide amine groups (NH_2) created dimethyl labels leading to mass shifts of
377 +28.0313 Da for the peptides from SerFA 3 h samples, +32.0564 Da for the peptides from SerFA-

378 Tric 6 h samples and +36.0757 for the peptides from SerFA-Tric 10 h samples respectively. The
379 three samples were mixed and then submitted to six rounds of phosphopeptide enrichment
380 with 5mg TiO_2 beads/mg of protein (Titansphere Phos-TiO, GL Sciences Inc., Netherlands) as
381 described (Soufi et al., 2018).

382 LC-MS/MS analyses of samples were done using an Ultimate 3000 nano-RSLC coupled on
383 line with a Q Exactive HF mass spectrometer (Thermo Scientific, San Jose California). 1 µL of
384 each sample was loaded on a C18 Acclaim PepMap100 trap-column 300 µm inner diameter (ID)
385 x 5 mm, 5 µm, 100Å, (Thermo Scientific) for 3.0 minutes at 20 µL/min with 2% acetonitrile
386 (ACN), 0.05% TFA in H_2O and then separated on a C18 Acclaim Pepmap100 nano-column, 50
387 cm x 75 µm ID, 2 µm, 100 Å (Thermo Scientific) with a 100 minute linear gradient from 3.2% to
388 20% buffer B (A: 0.1% FA in H_2O, B: 0.1% FA in ACN), from 20 to 32% of B in 20 min and then
389 from 32 to 90% of B in 2 min, hold for 10 min and returned to the initial conditions. The flow
390 rate was 300 nL/min.

391 Labeled peptides were analyzed with top15 higher energy collisional dissociation (HCD)
392 method: MS data were acquired in a data dependent strategy selecting the fragmentation
393 events based on the 15 most abundant precursor ions in the survey scan (m/z range from 350
394 to 1650). The resolution of the survey scan was 120,000 at m/z 200 Th and for MS/MS scan the
395 resolution was set to 15,000 at m/z 200 Th. For HCD acquisition, the collision energy = 27 and
396 the isolation width is of 1.4 m/z. The precursors with unknown charge state, charge state of 1
397 and 5 or greater than 5 were excluded. Peptides selected for MS/MS acquisition were then
398 placed on an exclusion list for 20 s using the dynamic exclusion mode to limit duplicate spectra.
399 The mass spectrometry proteomics data have been deposited to the Center for Computational
400 Mass Spectrometry repository (University of California, San Diego) *via* the MassIVE tool with
401 the dataset identifier MassIVE MSV000089781 (accessible at
402 http://massive.ucsd.edu/ProteoSAFe/status.jsp?task=db3f5002e32e4a47a71996358bc6ae8c
403).

404 **Phosphoproteome data analyses**. Proteins were identified by database searching using
405 SequestHT with Proteome Discoverer 2.5 software (Thermo Scientific, Fr) against the Uniprot
406 *S. aureus* USA300 database (2020-01 release, 2607 sequences). Precursor mass tolerance was
407 set at 10 ppm and fragment mass tolerance was set at 0.02 Da, and up to 2 missed cleavages
408 were allowed. Oxidation (M), acetylation (Protein N-terminus), and phosphorylation (S, T, Y)
409 were set as variable modifications. The differentially dimethyl-labeled peptides in primary
410 amino groups K and N-ter (see above), and carbamidomethylation (C) were set as fixed
411 modifications. Peptides and proteins were filtered with a false discovery rate (FDR) at 1% using
412 the Percolator tool (The et al., 2016). Protein quantitation was performed with precursor ions
413 quantifier node in Proteome Discoverer 2.5 software, peptide and protein quantitation based
414 on pairwise ratios and t-test statistical validation.
415 **Macrophage adhesion.** Confluent cell lawns of THP-1 macrophages were prepared as
416 described to obtain confluent cell lawns of $3x10^5$ cells per well (Bourrel et al., 2022). *S. aureus*
417 was pre-cultured in SerFA medium and then subcultured overnight in SerFA medium without
418 or with AFN-1252. The next day, bacteria were subcultured in the same corresponding fresh
419 media to OD_{600} =1-2. Bacteria were then washed twice with PBS buffer, and diluted in RPMI
420 GluMax (Gibco, France) to obtain an MOI = 1. One ml of the dilution was added in each well in
421 24-well plates. Plates were centrifuged at 1000 rpm for 5 minutes to sediment bacteria, and
422 then incubated at 4°C for 1h. After incubation, wells were washed 3 times with PBS, then 1ml
423 of sterile cold water was added to each well and left for 5min at room temperature. Finally, the
424 cells and bacteria were scraped from the surface and CFU were determined on SerFA agar
425 plates. Controls without macrophage were done in parallel. Results are derived from 5
426 biological replicates, and are presented as the mean ± standard error of the mean (SEM) using
427 GraphPad Prism 9.5.1 (San Diego, Ca). CFU counts were compared by paired t-test ($P<0.05$).
428 **Exoprotein activity assays.** SerFA day precultures were diluted into SerFA without or with
429 either triclosan (SerFA-Tric) and AFN-1252 (SerFA-AFN). Solid medium as prepared for

430 exoprotein detection were then spotted with resulting overnight saturated cultures or culture
431 supernatants as indicated. For nuclease detection, DNase agar (Oxoid, Thermo Scientific, Fr)
432 containing toluidine blue O 0.05 g/L (Sigma, Fr) was prepared as described (Zierdt and Golde,
433 1970). Culture supernatants from test samples were heated to 80°C for 10 m, and then spotted
434 (10 µl) on plates. Photographs were taken after overnight incubation at 37°C. Contrast was
435 uniformly enhanced by Photoshop to visualize pink halos indicating nuclease activity. To
436 measure protease activity, powdered skim milk 50 g/L was added to autoclaved 1% non-
437 nutrient agar (Invitrogen) as described (Park et al., 2012). Cultures were spotted (10 µl) on
438 plates and allowed to dry, then incubated at 37°C for 72 h and photographed. Lipase activity
439 was assayed in medium comprising 1% non-nutrient agar (Invitrogen) to which was added 2.5%
440 olive oil and 0.001% Rhodamine B (starting from a Rhodamine B stock solution of 1 mg per ml
441 in water; Sigma-Aldrich, Fr) as described (Araiza-Villanueva et al., 2019). To improve olive oil
442 emulsification, NaCl was added to medium (1M final concentration), followed by vigorous
443 shaking just prior to plate preparation. Supernatants from overnight cultures were sterile-
444 filtered through a 0.2 µm membrane syringe filter (Pall Corporation, Michigan). Supernatants
445 (10 µl) were deposited in holes pierced in solid medium. After 24 h incubation at 37°C plates
446 were visualized under UV light at 312 nm and photographed. Hemolytic activity was assayed
447 on *S. aureus* sterile-filtered supernatants that were prepared from overnight cultures. Aliquots
448 (10 µl) were spotted on 5% sheep blood agar plates (BioMérieux SA, Fr). After drying, plates
449 were incubated at 37°C overnight, and photographed.

450 **H_2O_2 resistance of non-treated and anti-FASII-adapted *S. aureus*.** *S. aureus* non-treated or
451 AFN-adapted cells (see above) were diluted to OD_{600}= 0.005 in SerFA and grown for 1 h at 37°C,
452 after which H_2O_2 (0.5mM final concentration) was added or not to cultures, and allowed to
453 grow for 5 h. Growth kinetics was followed by OD_{600} determinations, and CFUs were
454 determined at the final time point. Plates were photographed after overnight incubation at
455 37°C.

456 **H_2O_2 and PMS pre-treatment.** For pre-adaptation in hydrogen peroxide or in PMS, *S. aureus*
457 were precultured in SerFA and then subcultured in SerFA containing or not 0.5 mM H_2O_2 (final
458 concentration) or PMS (20-50 µM) for 16 h at 37°C. Cultures were diluted to OD_{600} = 0.1 in SerFA
459 or SerFA medium containing AFN-1252 (SerFA-AFN), and growth was monitored.
460 ***G. mellonella* infection by anti-FASII-adapted and untreated *S. aureus*.** Killing capacities and
461 CFUs of anti-FASII-adapted and untreated *S. aureus* USA300 were compared in the *G.*
462 *mellonella* insect model (Sheehan et al., 2019). *G. mellonella* larvae were reared on beeswax
463 and pollen in sealed containers with a wire mesh lid permitting aeration. The rearing container
464 was stored at 27°C temperature in a humidified incubator in our laboratory facilities. Fifth
465 instar larvae weighing ~250 mg were subjected to starvation for 24 h at 27°C and 1-2 h at 37°C
466 prior to infection. *S. aureus* SerFA cultures were subcultured in SerFA, and SerFA plus AFN-1252
467 (0.5 µg/ml; SerFA-AFN) for overnight growth. Resulting cultures were then diluted to 0.1 and
468 grown in respective media to OD_{600} = 1. Based on previous CFU determinations, each culture
469 was pelleted, washed once in PBS, and then resuspended in PBS to obtain 10^8 CFU/ml. Ten µl
470 (10^6 CFUs) was administered by injection in the fourth proleg. To follow larvae mortality
471 following *S. aureus* infection, 20 larvae were inoculated using 3 independent cultures per
472 culture condition (totaling 60 insects injected with SerFA, and 60 with SerFA-AFN), and 20
473 larvae were inoculated with PBS buffer for the control. Surviving larvae were counted every 24
474 h for 72 hours. To monitor *S. aureus* bacterial counts post-infection, the experiment above was
475 repeated, and surviving larvae (9 total per condition, treated in 3 groups from independent
476 biological replicates) were sacrificed until there were no surviving larvae left. CFUs were also
477 determined from newly-dead larvae. To determine *S. aureus* CFUs, surviving larvae were chilled
478 in ice for 30 min, and then crushed in 1 ml sterile deionized water. The resulting content was
479 vortexed for ~30 sec. Five µl of 10-fold dilutions were prepared in sterile water and spotted on
480 SerFA and SerFA-AFN solid media. CFUs were determined after overnight incubation at 37°C.
481 The detection threshold was 10^3 CFU per insect. Results of the 3 biologically independent

482 experiments were pooled for presentation of insect mortality, and similarly for CFUs as done
483 in the second independent experiment. Results are presented as the mean ± standard
484 deviation (SD) using GraphPad Prism 9.5.1 (San Diego, Ca). CFU counts were compared by
485 nonparametric t-test (Mann-Whitney U) ($P<0.05$). Note that *G. mellonella* naturally harbor
486 enterococci (Allonsius et al., 2019). In contrast to *S. aureus*, enterococci are catalase-negative
487 on routine plate tests (*n.b.*, some enterococci produce catalase upon heme addition). *S. aureus*
488 were thus differentiated from enterococci on plates used for CFU enumeration by their
489 catalase-positive response (*i.e.*, bubble formation) upon application of a 3% hydrogen peroxide
490 solution. Enterococci did not produce bubbles.
491

492 **Acknowledgments**

493 The Nebraska Transposon Mutant Library strains were generously provided by BEI Resources,
494 NIAID, NIH, USA, and by Dr. P. Fey (Nebraska Medical Center, Omaha, USA). We acknowledge
495 Micalis colleagues V. Sanchis and C. Nielson-LeRoux for valuable advice on the *G. mellonella*
496 infection model. We gratefully acknowledge our colleagues for their skillful technical assistance:
497 C. Buisson (Micalis) for insectarium and insect model, L. Dupont (Micalis) for proteomic sample
498 preparations, J. Guignot (Institut Cochin) for adhesion experiments, and F. Delolme (Université
499 de Lyon) for phosphoproteome studies. We thank P. Gaudu (Micalis) for valuable discussions.
500

501 **Funding**

502 We gratefully acknowledge funding support from the French National Research Agency
503 StaphEscape project 16CE150013 (AG, CG, AF), the Fondation pour la Recherche Medicale
504 (DBF20161136769)(AG), and DIM One Health (RPH17043DJA) (AF). PW received a Franco-Thai
505 scholarship from Campus France and Khon Kaen University. JPL and CG acknowledge financial
506 support from the CNRS and the ITMO Cancer AVIESAN (Alliance Nationale pour les Sciences de
507 la Vie et de la Santé, National Alliance for Life Sciences and Health) within the framework of the

cancer plan for Orbitrap mass spectrometer funding. Phosphoproteomes were performed at the Protein Science Facility, SFR BioSciences CNRS UAR3444, Inserm US8, UCBL, ENS de Lyon, 50 Avenue Tony Garnier, 69007 Lyon, Fr.

Data Availability

All relevant data are within the manuscript, supporting information files, and depositories.

Competing interests

The authors declare that no competing interests exist.

519 **References**

520 ALBANESI, D., REH, G., GUERIN, M. E., SCHAEFFER, F., DEBARBOUILLE, M., BUSCHIAZZO, A.,
521 SCHUJMAN, G. E., DE MENDOZA, D. & ALZARI, P. M. 2013. Structural basis for feed-forward
522 transcriptional regulation of membrane lipid homeostasis in *Staphylococcus aureus*. *PLoS*
523 *Pathog,* 9**,** e1003108.
524 ALLONSIUS, C. N., VAN BEECK, W., DE BOECK, I., WITTOUCK, S. & LEBEER, S. 2019. The
525 microbiome of the invertebrate model host Galleria mellonella is dominated by
526 Enterococcus. *Anim Microbiome,* 1**,** 7.
527 ALNASERI, H., ARSIC, B., SCHNEIDER, J. E., KAISER, J. C., SCINOCCA, Z. C., HEINRICHS, D. E. &
528 MCGAVIN, M. J. 2015. Inducible Expression of a Resistance-Nodulation-Division-Type Efflux
529 Pump in *Staphylococcus aureus* Provides Resistance to Linoleic and Arachidonic Acids. *J*
530 *Bacteriol,* 197**,** 1893-905.
531 ARAIZA-VILLANUEVA, M., AVILA-CALDERON, E. D., FLORES-ROMO, L., CALDERON-AMADOR, J.,
532 SRIRANGANATHAN, N., QUBLAN, H. A., WITONSKY, S., AGUILERA-ARREOLA, M. G., RUIZ-
533 PALMA, M. D. S., RUIZ, E. A., SUAREZ-GUEMES, F., GOMEZ-LUNAR, Z. & CONTRERAS-
534 RODRIGUEZ, A. 2019. Proteomic Analysis of Membrane Blebs of Brucella abortus 2308 and
535 RB51 and Their Evaluation as an Acellular Vaccine. *Front Microbiol,* 10**,** 2714.
536 BEDNARZ, B., MILLAN-OROPEZA, A., KOTOWSKA, M., SWIAT, M., QUISPE HARO, J. J., HENRY, C.
537 & PAWLIK, K. 2021. Coelimycin Synthesis Activatory Proteins Are Key Regulators of
538 Specialized Metabolism and Precursor Flux in *Streptomyces coelicolor* A3(2). *Front Microbiol,*
539 12**,** 616050.
540 BOERSEMA, P. J., RAIJMAKERS, R., LEMEER, S., MOHAMMED, S. & HECK, A. J. 2009. Multiplex
541 peptide stable isotope dimethyl labeling for quantitative proteomics. *Nat Protoc,* 4**,** 484-94.
542 BOURREL, A. S., PICART, A., FERNANDEZ, J. C., HAYS, C., SAUBAMEA, B., MIGNON, V., POYART,
543 C., TAZI, A. & GUIGNOT, J. 2022. Specific interaction between Group B Streptococcus CC17
544 hypervirulent clone and phagocytes. *BioRxiv*.
545 BRINSTER, S., LAMBERET, G., STAELS, B., TRIEU-CUOT, P., GRUSS, A. & POYART, C. 2009. Type II
546 fatty acid synthesis is not a suitable antibiotic target for Gram-positive pathogens. *Nature,*
547 458**,** 83-6.
548 BURY-MONE, S., NOMANE, Y., REYMOND, N., BARBET, R., JACQUET, E., IMBEAUD, S., JACQ, A. &
549 BOULOC, P. 2009. Global analysis of extracytoplasmic stress signaling in *Escherichia coli*. *PLoS*
550 *Genet,* 5**,** e1000651.
551 COLE, J., ABERDEIN, J., JUBRAIL, J. & DOCKRELL, D. H. 2014. The role of macrophages in the innate
552 immune response to *Streptococcus pneumoniae* and *Staphylococcus aureus*: mechanisms
553 and contrasts. *Adv Microb Physiol,* 65**,** 125-202.
554 CUSUMANO, J. A., KLINKER, K. P., HUTTNER, A., LUTHER, M. K., ROBERTS, J. A. & LAPLANTE, K. L.
555 2020. Towards precision medicine: Therapeutic drug monitoring-guided dosing of
556 vancomycin and beta-lactam antibiotics to maximize effectiveness and minimize toxicity. *Am*
557 *J Health Syst Pharm,* 77**,** 1104-1112.
558 DECOURSEY, T. E. 2004. During the respiratory burst, do phagocytes need proton channels or
559 potassium channels, or both? *Sci STKE,* 2004**,** pe21.
560 DEROUICHE, A., BIDNENKO, V., GRENHA, R., PIGONNEAU, N., VENTROUX, M., FRANZ-WACHTEL,
561 M., NESSLER, S., NOIROT-GROS, M. F. & MIJAKOVIC, I. 2013. Interaction of bacterial fatty-
562 acid-displaced regulators with DNA is interrupted by tyrosine phosphorylation in the helix-
563 turn-helix domain. *Nucleic Acids Res,* 41**,** 9371-81.
564 DYZENHAUS, S., SULLIVAN, M. J., ALBURQUERQUE, B., BOFF, D., VAN DE GUCHTE, A., CHUNG,
565 M., FULMER, Y., COPIN, R., ILMAIN, J. K., O'KEEFE, A., ALTMAN, D. R., STUBBE, F. X.,
566 PODKOWIK, M., DUPPER, A. C., SHOPSIN, B., VAN BAKEL, H. & TORRES, V. J. 2022. MRSA
567 lineage USA300 isolated from bloodstream infections exhibit altered virulence regulation.
568 *Cell Host Microbe*.

FAGE, C. D., LATHOUWERS, T., VANMEERT, M., GAO, L. J., VRANCKEN, K., LAMMENS, E. M., WEIR, A. N. M., DEGROOTE, R., CUPPENS, H., KOSOL, S., SIMPSON, T. J., CRUMP, M. P., WILLIS, C. L., HERDEWIJN, P., LESCRINIER, E., LAVIGNE, R., ANNE, J. & MASSCHELEIN, J. 2020. The Kalimantacin Polyketide Antibiotics Inhibit Fatty Acid Biosynthesis in *Staphylococcus aureus* by Targeting the Enoyl-Acyl Carrier Protein Binding Site of FabI. *Angew Chem Int Ed Engl,* 59**,** 10549-10556.

FEY, P. D., ENDRES, J. L., YAJJALA, V. K., WIDHELM, T. J., BOISSY, R. J., BOSE, J. L. & BAYLES, K. W. 2013. A genetic resource for rapid and comprehensive phenotype screening of nonessential *Staphylococcus aureus* genes. *MBio,* 4**,** e00537-12.

GARCIA-GARCIA, T., PONCET, S., DEROUICHE, A., SHI, L., MIJAKOVIC, I. & NOIROT-GROS, M. F. 2016. Role of Protein Phosphorylation in the Regulation of Cell Cycle and DNA-Related Processes in Bacteria. *Front Microbiol,* 7**,** 184.

GERSTEL, A., ZAMARRENO BEAS, J., DUVERGER, Y., BOUVERET, E., BARRAS, F. & PY, B. 2020. Oxidative stress antagonizes fluoroquinolone drug sensitivity via the SoxR-SUF Fe-S cluster homeostatic axis. *PLoS Genet,* 16**,** e1009198.

GLOUX, K., GUILLEMET, M., SOLER, C., MORVAN, C., HALPERN, D., POURCEL, C., VU THIEN, H., LAMBERET, G. & GRUSS, A. 2017. Clinical Relevance of Type II Fatty Acid Synthesis Bypass in *Staphylococcus aureus*. *Antimicrob Agents Chemother,* 61**,** 61:e02515-16.

HUANG, L., MATSUO, M., CALDERON, C., FAN, S. H., AMMANATH, A. V., FU, X., LI, N., LUQMAN, A., ULLRICH, M., HERRMANN, F., MAIER, M., CHENG, A., ZHANG, F., OESTERHELT, F., LAMMERHOFER, M. & GOTZ, F. 2022. Molecular Basis of Rhodomyrtone Resistance in *Staphylococcus aureus*. *mBio***,** e0383321.

HUNT, T., KAPLAN, N. & HAFKIN, B. 2016. Safety, tolerability and pharmacokinetics of multiple oral doses of AFN-1252 administered as immediate release (IR) tablets in healthy subjects. *J Chemother,* 28**,** 164-71.

JI, C. J., KIM, J. H., WON, Y. B., LEE, Y. E., CHOI, T. W., JU, S. Y., YOUN, H., HELMANN, J. D. & LEE, J. W. 2015. *Staphylococcus aureus* PerR Is a Hypersensitive Hydrogen Peroxide Sensor using Iron-mediated Histidine Oxidation. *J Biol Chem,* 290**,** 20374-86.

KARLOWSKY, J. A., KAPLAN, N., HAFKIN, B., HOBAN, D. J. & ZHANEL, G. G. 2009. AFN-1252, a FabI inhibitor, demonstrates a Staphylococcus-specific spectrum of activity. *Antimicrob Agents Chemother,* 53**,** 3544-8.

KAZEK, M., KACZMAREK, A., WRONSKA, A. K. & BOGUS, M. I. 2021. Dodecanol, metabolite of entomopathogenic fungus Conidiobolus coronatus, affects fatty acid composition and cellular immunity of Galleria mellonella and Calliphora vicina. *Sci Rep,* 11**,** 15963.

KENANIAN, G., MORVAN, C., WECKEL, A., PATHANIA, A., ANBA-MONDOLONI, J., HALPERN, D., GAILLARD, M., SOLGADI, A., DUPONT, L., HENRY, C., POYART, C., FOUET, A., LAMBERET, G., GLOUX, K. & GRUSS, A. 2019. Permissive Fatty Acid Incorporation Promotes Staphylococcal Adaptation to FASII Antibiotics in Host Environments. *Cell Rep,* 29**,** 3974-3982 e4.

KHEMICI, V., PRADOS, J., PETRIGNANI, B., DI NOLFI, B., BERGE, E., MANZANO, C., GIRAUD, C. & LINDER, P. 2020. The DEAD-box RNA helicase CshA is required for fatty acid homeostasis in *Staphylococcus aureus*. *PLoS Genet,* 16**,** e1008779.

LAKHUNDI, S. & ZHANG, K. 2018. Methicillin-Resistant *Staphylococcus aureus*: Molecular Characterization, Evolution, and Epidemiology. *Clin Microbiol Rev,* 31.

LAMBERT, C., BACHMANN, C., GAILLARD, M., HAUTCOEUR, A., GLOUX, K., GUILBERT, T., MÉHATS, C., PROST, B., SOLGADI, A., ABREU, S., ANDRIEU, M., POYART, C., GRUSS, A. & FOUET, A. 2023. *Streptococcus pyogenes* FASII regulator FabT is required for human tissue infection but is a negative fitness determinant in lipid-rich biotopes. *Submitted*.

LAMBERT, C., POYART, C., GRUSS, A. & FOUET, A. 2022. FabT, a Bacterial Transcriptional Repressor That Limits Futile Fatty Acid Biosynthesis. *Microbiol Mol Biol Rev,* 86**,** e0002922.

LEI, M. G. & LEE, C. Y. 2018. Repression of Capsule Production by XdrA and CodY in *Staphylococcus aureus*. *J Bacteriol,* 200.

620 LIU, G. Y., ESSEX, A., BUCHANAN, J. T., DATTA, V., HOFFMAN, H. M., BASTIAN, J. F., FIERER, J. &
621 NIZET, V. 2005. *Staphylococcus aureus* golden pigment impairs neutrophil killing and
622 promotes virulence through its antioxidant activity. *J Exp Med,* 202**,** 209-15.
623 LOPEZ, M. S., TAN, I. S., YAN, D., KANG, J., MCCREARY, M., MODRUSAN, Z., AUSTIN, C. D., XU, M.
624 & BROWN, E. J. 2017. Host-derived fatty acids activate type VII secretion in *Staphylococcus*
625 *aureus*. *Proc Natl Acad Sci U S A,* 114**,** 11223-11228.
626 LOWDEN, M. J., SKORUPSKI, K., PELLEGRINI, M., CHIORAZZO, M. G., TAYLOR, R. K. & KULL, F. J.
627 2010. Structure of Vibrio cholerae ToxT reveals a mechanism for fatty acid regulation of
628 virulence genes. *Proc Natl Acad Sci U S A,* 107**,** 2860-5.
629 LOWY, F. D. 1998. *Staphylococcus aureus* infections. *N Engl J Med,* 339**,** 520-32.
630 MAYER-SCHOLL, A., AVERHOFF, P. & ZYCHLINSKY, A. 2004. How do neutrophils and pathogens
631 interact? *Curr Opin Microbiol,* 7**,** 62-6.
632 MCCALLUM, N., HINDS, J., ENDER, M., BERGER-BACHI, B. & STUTZMANN MEIER, P. 2010.
633 Transcriptional profiling of XdrA, a new regulator of spa transcription in *Staphylococcus*
634 *aureus*. *J Bacteriol,* 192**,** 5151-64.
635 MCMURRY, L. M., OETHINGER, M. & LEVY, S. B. 1998. Triclosan targets lipid synthesis. *Nature,*
636 394**,** 531-2.
637 MIJAKOVIC, I., GRANGEASSE, C. & TURGAY, K. 2016. Exploring the diversity of protein
638 modifications: special bacterial phosphorylation systems. *FEMS Microbiol Rev,* 40**,** 398-417.
639 MORVAN, C., HALPERN, D., KENANIAN, G., HAYS, C., ANBA-MONDOLONI, J., BRINSTER, S.,
640 KENNEDY, S., TRIEU-CUOT, P., POYART, C., LAMBERET, G., GLOUX, K. & GRUSS, A. 2016.
641 Environmental fatty acids enable emergence of infectious *Staphylococcus aureus* resistant to
642 FASII-targeted antimicrobials. *Nat Commun,* 7**,** 12944.
643 MORVAN, C., HALPERN, D., KENANIAN, G., PATHANIA, A., ANBA-MONDOLONI, J., LAMBERET, G.,
644 GRUSS, A. & GLOUX, K. 2017. The *Staphylococcus aureus* FASII bypass escape route from FASII
645 inhibitors. *Biochimie,* 141**,** 40-46.
646 MOSEL, M., LI, L., DRLICA, K. & ZHAO, X. 2013. Superoxide-mediated protection of *Escherichia*
647 *coli* from antimicrobials. *Antimicrob Agents Chemother,* 57**,** 5755-9.
648 PAINTER, K. L., STRANGE, E., PARKHILL, J., BAMFORD, K. B., ARMSTRONG-JAMES, D. & EDWARDS,
649 A. M. 2015. *Staphylococcus aureus* adapts to oxidative stress by producing H2O2-resistant
650 small-colony variants via the SOS response. *Infect Immun,* 83**,** 1830-44.
651 PARK, J. H., LEE, J. H., CHO, M. H., HERZBERG, M. & LEE, J. 2012. Acceleration of protease effect
652 on *Staphylococcus aureus* biofilm dispersal. *FEMS Microbiol Lett,* 335**,** 31-8.
653 PARKER, E. N., CAIN, B. N., HAJIAN, B., ULRICH, R. J., GEDDES, E. J., BARKHO, S., LEE, H. Y.,
654 WILLIAMS, J. D., RAYNOR, M., CARIDHA, D., ZAINO, A., SHEKHAR, M., MUNOZ, K. A., RZASA,
655 K. M., TEMPLE, E. R., HUNT, D., JIN, X., VUONG, C., PANNONE, K., KELLY, A. M., MULLIGAN,
656 M. P., LEE, K. K., LAU, G. W., HUNG, D. T. & HERGENROTHER, P. J. 2022. An Iterative Approach
657 Guides Discovery of the FabI Inhibitor Fabimycin, a Late-Stage Antibiotic Candidate with In
658 Vivo Efficacy against Drug-Resistant Gram-Negative Infections. *ACS Cent Sci,* 8**,** 1145-1158.
659 PARSONS, J. B., BROUSSARD, T. C., BOSE, J. L., ROSCH, J. W., JACKSON, P., SUBRAMANIAN, C. &
660 ROCK, C. O. 2014. Identification of a two-component fatty acid kinase responsible for host
661 fatty acid incorporation by *Staphylococcus aureus*. *Proc Natl Acad Sci U S A,* 111**,** 10532-7.
662 PARSONS, J. B., FRANK, M. W., SUBRAMANIAN, C., SAENKHAM, P. & ROCK, C. O. 2011. Metabolic
663 basis for the differential susceptibility of Gram-positive pathogens to fatty acid synthesis
664 inhibitors. *Proc Natl Acad Sci U S A,* 108**,** 15378-83.
665 PATHANIA, A., ANBA-MONDOLONI, J., GOMINET, M., HALPERN, D., DAIROU, J., DUPONT, L.,
666 LAMBERET, G., TRIEU-CUOT, P., GLOUX, K. & GRUSS, A. 2021. (p)ppGpp/GTP and Malonyl-
667 CoA Modulate *Staphylococcus aureus* Adaptation to FASII Antibiotics and Provide a Basis for
668 Synergistic Bi-Therapy. *mBio,* 12.
669 PEYRUSSON, F., NGUYEN, T. K., NAJDOVSKI, T. & VAN BAMBEKE, F. 2022. Host Cell Oxidative
670 Stress Induces Dormant *Staphylococcus aureus* Persisters. *Microbiol Spectr,* 10**,** e0231321.

671 PISHCHANY, G., MEVERS, E., NDOUSSE-FETTER, S., HORVATH, D. J., JR., PALUDO, C. R., SILVA-
672 JUNIOR, E. A., KOREN, S., SKAAR, E. P., CLARDY, J. & KOLTER, R. 2018. Amycomicin is a potent
673 and specific antibiotic discovered with a targeted interaction screen. *Proc Natl Acad Sci U S*
674 *A,* 115**,** 10124-10129.
675 RASIGADE, J. P. & VANDENESCH, F. 2014. *Staphylococcus aureus*: a pathogen with still
676 unresolved issues. *Infect Genet Evol,* 21**,** 510-4.
677 ROBERTS, C. A., AL-TAMEEMI, H. M., MASHRUWALA, A. A., ROSARIO-CRUZ, Z., CHAUHAN, U.,
678 SAUSE, W. E., TORRES, V. J., BELDEN, W. J. & BOYD, J. M. 2017. The Suf Iron-Sulfur Cluster
679 Biosynthetic System Is Essential in *Staphylococcus aureus*, and Decreased Suf Function
680 Results in Global Metabolic Defects and Reduced Survival in Human Neutrophils. *Infect*
681 *Immun,* 85.
682 SCHURIG-BRICCIO, L. A., PARRAGA SOLORZANO, P. K., LENCINA, A. M., RADIN, J. N., CHEN, G. Y.,
683 SAUER, J. D., KEHL-FIE, T. E. & GENNIS, R. B. 2020. Role of respiratory NADH oxidation in the
684 regulation of *Staphylococcus aureus* virulence. *EMBO Rep,* 21**,** e45832.
685 SENDI, P. & PROCTOR, R. A. 2009. *Staphylococcus aureus* as an intracellular pathogen: the role
686 of small colony variants. *Trends Microbiol,* 17**,** 54-8.
687 SHEEHAN, G., DIXON, A. & KAVANAGH, K. 2019. Utilization of Galleria mellonella larvae to
688 characterize the development of *Staphylococcus aureus* infection. *Microbiology (Reading),*
689 165**,** 863-875.
690 SOUFI, B., TAUMER, C., SEMANJSKI, M. & MACEK, B. 2018. Phosphopeptide Enrichment from
691 Bacterial Samples Utilizing Titanium Oxide Affinity Chromatography. *Methods Mol Biol,* 1841**,**
692 231-247.
693 STAPLETON, M. R., HORSBURGH, M. J., HAYHURST, E. J., WRIGHT, L., JONSSON, I. M.,
694 TARKOWSKI, A., KOKAI-KUN, J. F., MOND, J. J. & FOSTER, S. J. 2007. Characterization of IsaA
695 and SceD, two putative lytic transglycosylases of *Staphylococcus aureus*. *J Bacteriol,* 189**,**
696 7316-25.
697 THE, M., MACCOSS, M. J., NOBLE, W. S. & KALL, L. 2016. Fast and Accurate Protein False
698 Discovery Rates on Large-Scale Proteomics Data Sets with Percolator 3.0. *J Am Soc Mass*
699 *Spectrom,* 27**,** 1719-1727.
700 TUCHSCHERR, L., LOFFLER, B. & PROCTOR, R. A. 2020. Persistence of *Staphylococcus aureus*:
701 Multiple Metabolic Pathways Impact the Expression of Virulence Factors in Small-Colony
702 Variants (SCVs). *Front Microbiol,* 11**,** 1028.
703 WANG, J., SOISSON, S. M., YOUNG, K., SHOOP, W., KODALI, S., GALGOCI, A., PAINTER, R.,
704 PARTHASARATHY, G., TANG, Y. S., CUMMINGS, R., HA, S., DORSO, K., MOTYL, M.,
705 JAYASURIYA, H., ONDEYKA, J., HERATH, K., ZHANG, C., HERNANDEZ, L., ALLOCCO, J., BASILIO,
706 A., TORMO, J. R., GENILLOUD, O., VICENTE, F., PELAEZ, F., COLWELL, L., LEE, S. H., MICHAEL,
707 B., FELCETTO, T., GILL, C., SILVER, L. L., HERMES, J. D., BARTIZAL, K., BARRETT, J., SCHMATZ,
708 D., BECKER, J. W., CULLY, D. & SINGH, S. B. 2006. Platensimycin is a selective FabF inhibitor
709 with potent antibiotic properties. *Nature,* 441**,** 358-61.
710 WRIGHT, H. T. & REYNOLDS, K. A. 2007. Antibacterial targets in fatty acid biosynthesis. *Curr Opin*
711 *Microbiol,* 10**,** 447-53.
712 WU, Y., VULIC, M., KEREN, I. & LEWIS, K. 2012. Role of oxidative stress in persister tolerance.
713 *Antimicrob Agents Chemother,* 56**,** 4922-6.
714 YAO, J. & ROCK, C. O. 2016. Resistance Mechanisms and the Future of Bacterial Enoyl-Acyl Carrier
715 Protein Reductase (FabI) Antibiotics. *Cold Spring Harb Perspect Med,* 6**,** a027045.
716 YEO, W. S., DYZENHAUS, S., TORRES, V. J., BRINSMADE, S. R. & BAE, T. 2023. Regulation of
717 Bacterial Two-Component Systems by Cardiolipin. *BioRxiv*.
718 ZHANG, Y. M. & ROCK, C. O. 2008. Membrane lipid homeostasis in bacteria. *Nat Rev Microbiol,*
719 6**,** 222-33.
720 ZIERDT, C. H. & GOLDE, D. W. 1970. Deoxyribonuclease-positive *Staphylococcus epidermidis*
721 strains. *Appl Microbiol,* 20**,** 54-7.

722 **Table 1. Pre-treatments with ROS-generating *versus* reducing agents respectively accelerate**
723 **and retard adaptation to anti-FASII.**
724
725

Strain [a]	Additive [b]	Time (h) to exit	Δ anti-FASII exit (h) compared to WT (SD) [c]	N
WT	-	8	-	8
WT	H_2O_2	6.3	+ 1.68 (±0.45)	8
WT	PMS	6.5	+ 1.50 (±0.35)	5
katA	-	7	+ 1.00 (±0.00)	3
katA	H_2O_2	5.8	+ 2.17 (±0.58)	3
perR	-	9	- 1.00 (±0.00)	3
perR	H_2O_2	9	- 1.00 (±0.00)	3
*sufD**	-	7.3	+ 0.75 (±0.50)	4
*sufD**	H_2O_2	6.7	+ 1.25 (±0.29)	4
WT	Na citrate	11.5	- 3.50 (±0.71)	2
WT	Vit C	9.8	- 1.75 (±0.35)	2

726
727
728
729 [a] Strains USA300 (WT) or mutant derivatives *katA* SAUSA300_1232, *perR* SAUSA300_1842, or
730 *sufD** intergenic between *sufC* (SAUSA300_0818) and *sufD* (SAUSA300_0819), at position
731 898566 (Fey et al., 2013, Roberts et al., 2017), are used. [b] Oxidizing agents were added only to
732 precultures: H_2O_2, 0.5 mM; phenazine-methosulfate (PMS), 20 (n=2), 30 (n=1), 40 (n=1), 50 (n=1)
733 µg/ml, gave equivalent results. Reducing agents were added at the same time as anti-FASII, here
734 AFN-1252: sodium citrate, 10 mM; vitamin C (VitC), 5.7 mM. [c] Bacterial outgrowth for USA300 in
735 SerFA-AFN is observed at 8 h, and is used as reference. Differences (Δ) in time of outgrowth are
736 relative to that of the WT. +, early exit from latency (h); -, delayed exit (h). SD, standard
737 deviation; N, number of independent experiments.
738
739

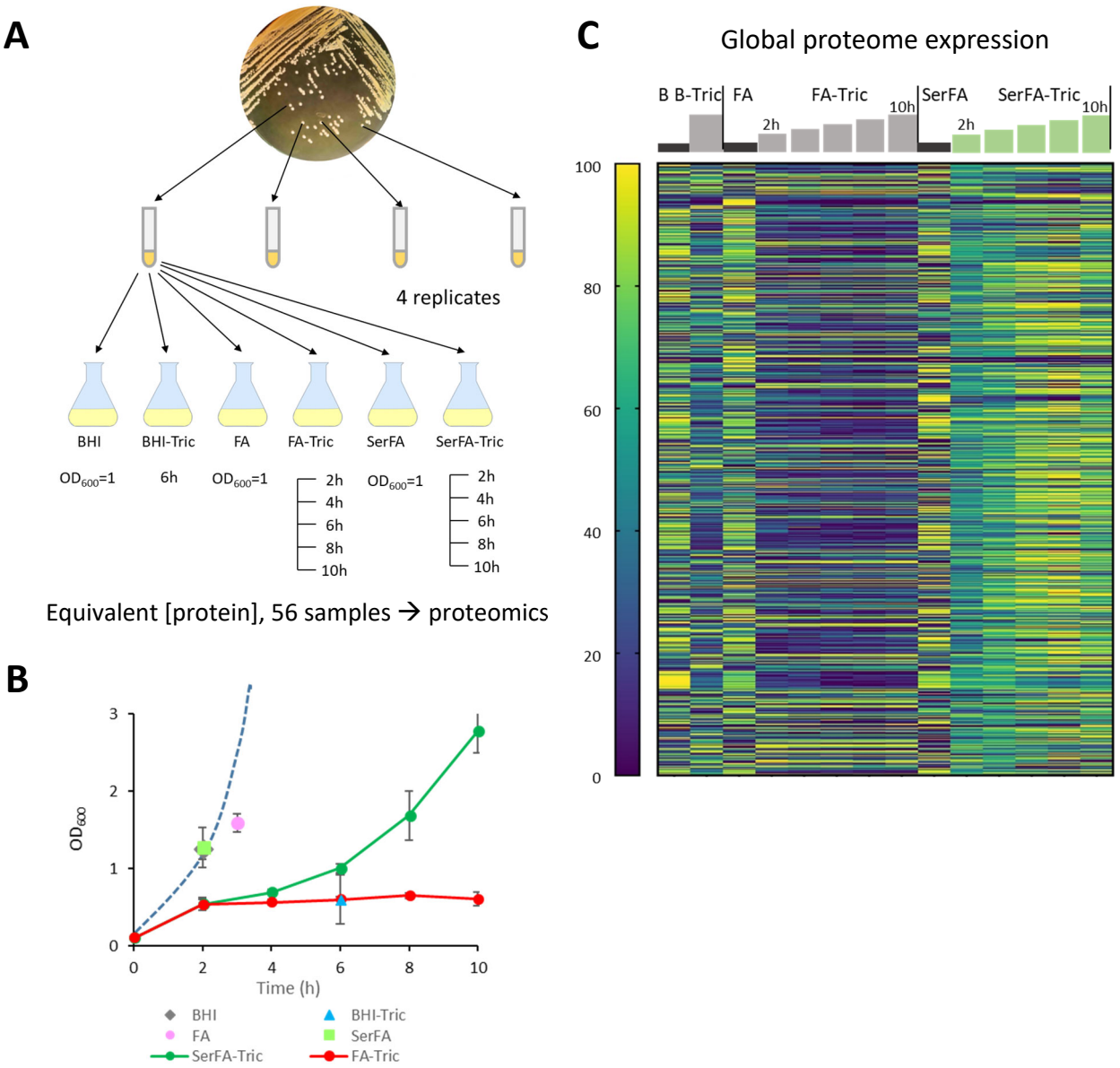

Fig. 1. Proteomic kinetics and global expression changes related to *S. aureus* USA300 strain adaptation to anti-FASII. A. Schematics of sample preparation. Samples (4 biological replicates) were grown and prepared in conditions and harvesting times (or OD_{600} for controls) as indicated below flasks. **B. Sample growth.** Means and standard deviations are indicated. Points correspond to sampling times. See **Table S1** for details. Dashed blue line represents typical growth in SerFA medium determined separately. *S. aureus* adapts to anti-FASII within 10h on SerFA-Tric, but not on FA-Tric, after a latency period (double arrow). **C. Heat map of proteins showing altered levels in at least 1 condition relative to other samples.** All sample conditions are shown. Sampling times (h) above steps correspond to 2, 4, 6, 8, and 10 h for FA-Tric and SerFA-Tric. The heat map shows global protein changes, and is determined relative to weighted value for each protein, as on scale at left (navy, down-represented; yellow, up-represented).

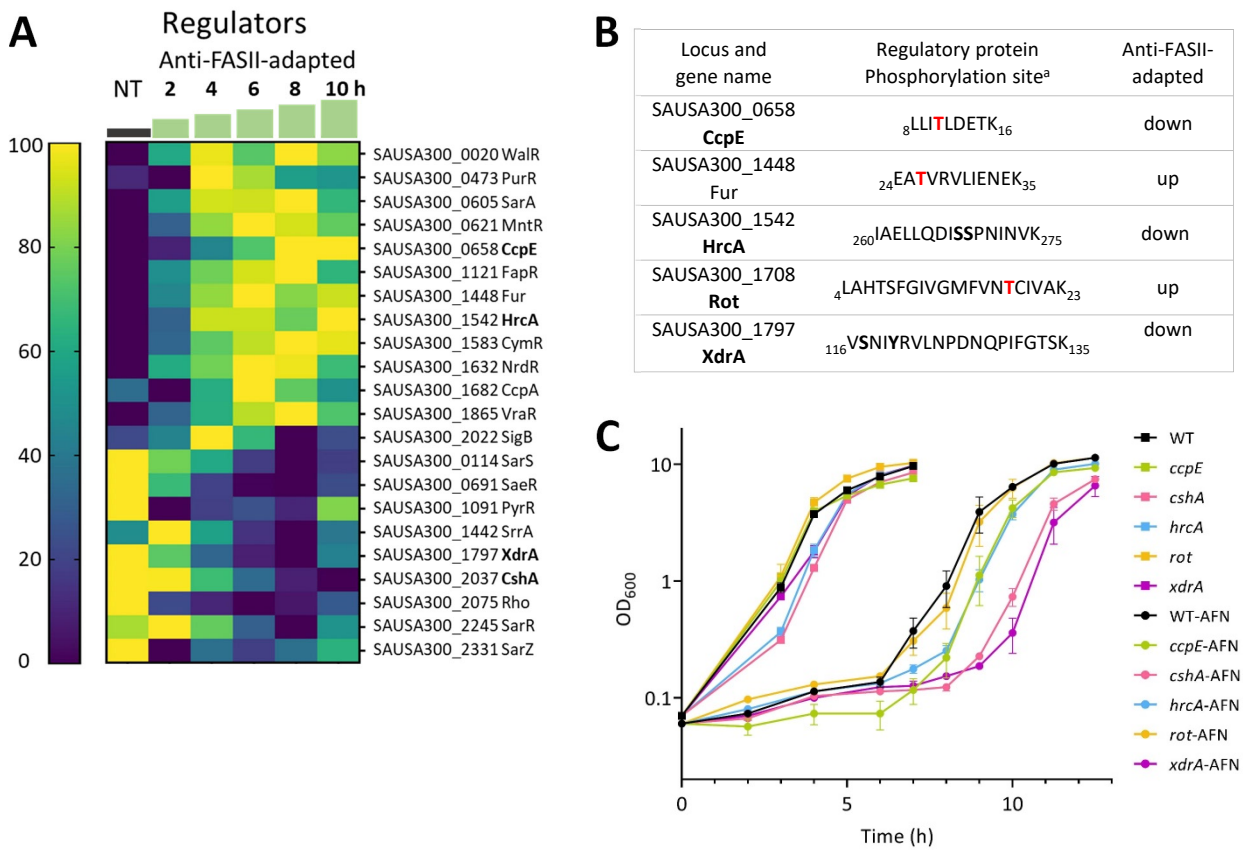

Locus and gene name	Regulatory protein Phosphorylation site[a]	Anti-FASII-adapted
SAUSA300_0658 **CcpE**	$_{8}$LLI**T**LDETK$_{16}$	down
SAUSA300_1448 Fur	$_{24}$EA**T**VRVLIENEK$_{35}$	up
SAUSA300_1542 **HrcA**	$_{260}$IAELLQDI**SS**PNINVK$_{275}$	down
SAUSA300_1708 **Rot**	$_{4}$LAHTSFGIVGMFVN**T**CIVAK$_{23}$	up
SAUSA300_1797 **XdrA**	$_{116}$V**S**NI**Y**RVLNPDNQPIFGTSK$_{135}$	down

Fig. 2. Anti-FASII affects pools and phosphorylation status of regulatory proteins. A. Expression of known or putative regulators that differ in at least one time point during anti-FASII adaptation (SerFA-Tric) compared to non-treated (NT) SerFA sample. Changes in putative regulatory protein levels are shown in anti-FASII adaptation SerFA medium (see **Table S1** for all test conditions). Gene loci and names are at right. Times (h) of sampling are indicated above green steps. Heat map (scale at left) is determined relative to weighted value for each protein (navy, down-represented; yellow, up-represented). **B**. **Phosphorylated regulatory proteins with altered expression during anti-FASII adaptation.** Peptides showing differential phosphorylation at 10 h post anti-FASII adaptation are indicated (see **Table S2** for complete information). [a] Peptide positions in respective protein sequences are indicated. Phosphorylated amino acids are in bold red or in bold black when there is an ambiguity. **C. Effects of regulator gene inactivation on anti-FASII adaptation.** Kinetics of anti-FASII-adaptation of USA300 (WT) and insertional mutants, based on regulators with altered protein and/or phosphorylation levels (**A** and/or **B**; selected loci in bold), were compared to that of the parental strain. Cultures were grown without (squares) and with anti-FASII AFN-1252 (circles). Growth curves and standard deviations are based on biological triplicates.

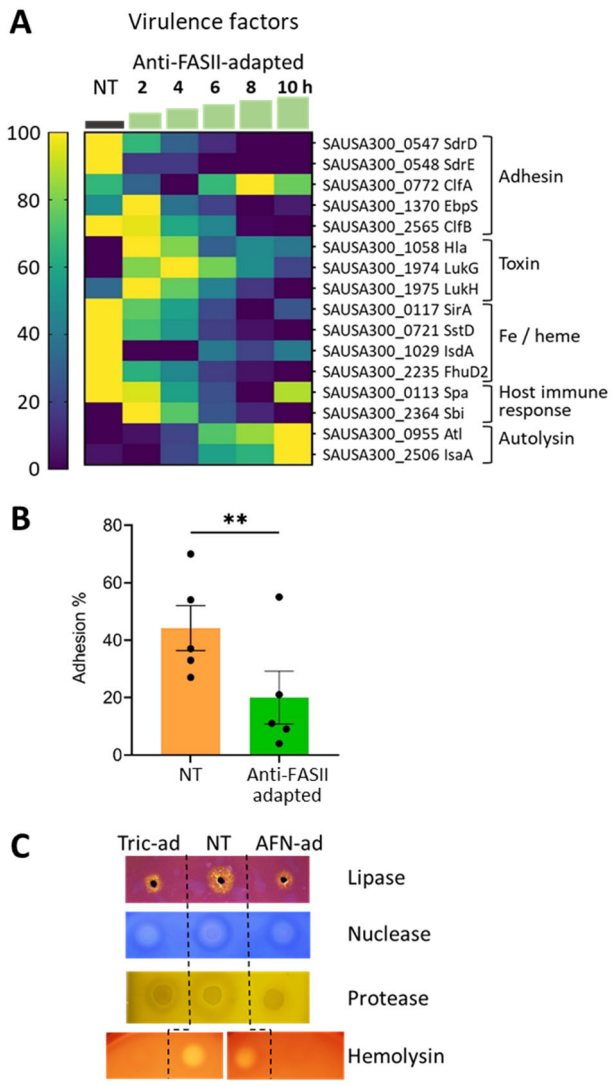

Fig. 3. Expression changes during anti-FASII treatment. A. Heat maps of known or putative virulence factors. Samples shown are in anti-FASII adaptation medium (SerFA; see **Table S1** for results in all test conditions). Kinetics (in h) of sampling is indicated above green steps. Gene loci, protein names, and functional categories are at right. Correspondence between color and expression in heat map (scale at left) is determined relative to weighted value for each protein (navy, down-represented; yellow, up-represented). **B. Differential NT and anti-FASII-adapted *S. aureus* adhesion to macrophage.** Non-treated (NT) or AFN-1252-treated *S. aureus* USA300 ($3x10^5$) were added to of THP-1 macrophage monolayers ($3x10^5$ cells per well), and incubated for 1 h at 4° C. Colony forming units (CFU) of bacteria that adhered to macrophage were determined on five independent bacterial samples (P= 0.003; see Materials and Methods). **C. Secreted virulence factor activities.** Non-treated (NT) and anti-FASII-adapted cultures treated with triclosan (Tric-ad) or AFN-1252 (AFN-ad) were grown overnight, and reached similar OD_{600} values (= 13, 9 and 9 respectively for NT, Tric-ad, and AFN-ad). Cultures (for protease detection) and culture supernatants (lipase, nuclease, and hemolysin detection) were prepared (see Materials and Methods) and spotted on appropriate detection medium. Representative results of 3 biologically independent replicates are shown.

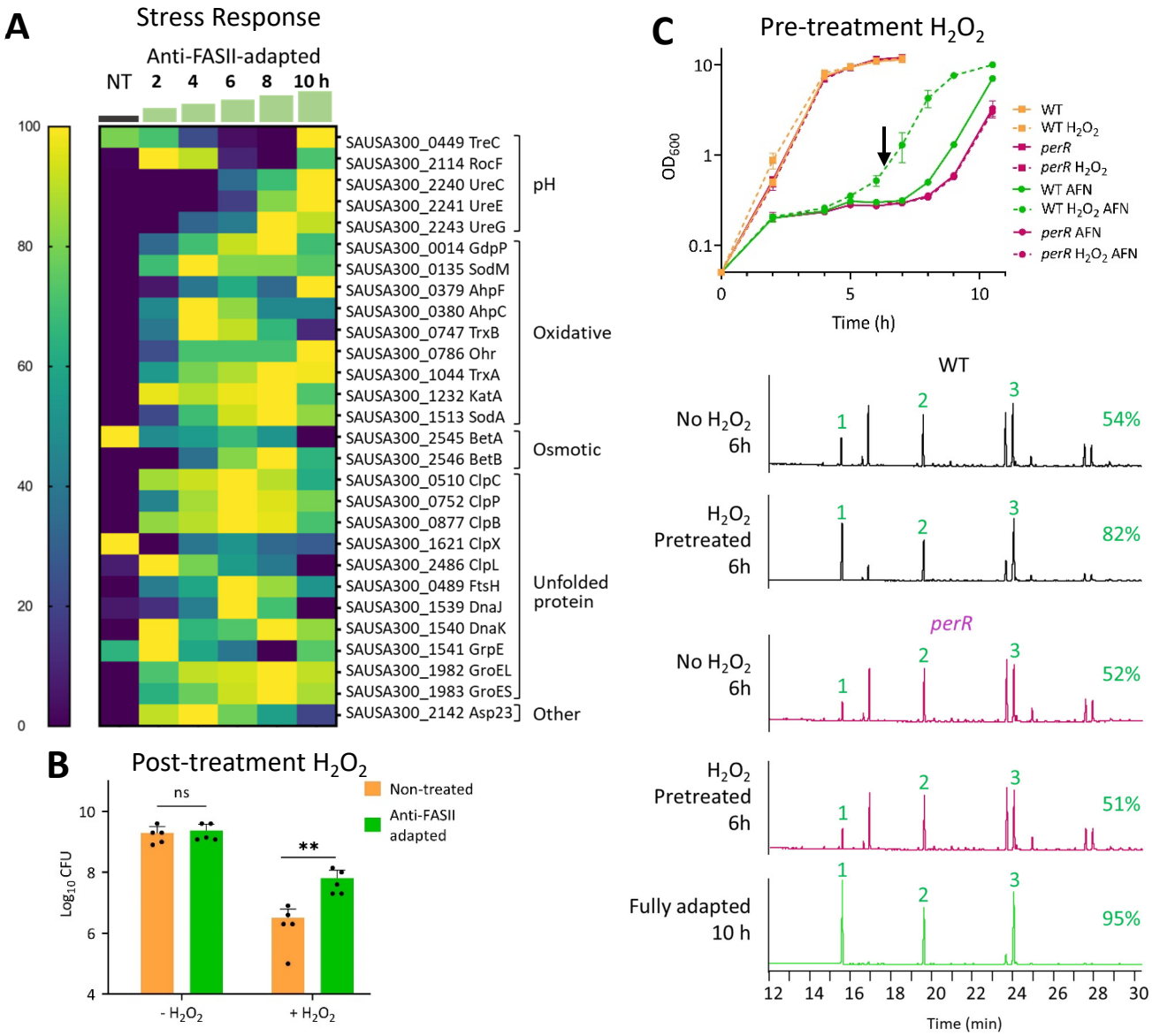

Fig. 4. Anti-FASII adaptation confers oxidative stress resistance, and is accelerated by prior exposure to peroxide stress. A. Stress response heatmap. Results are shown for anti-FASII adaptation medium (SerFA; see **Table S1** for all test conditions). Sampling times (h) are indicated above green steps. Gene names and functional categories are at right. Heat map (scale at left) is determined relative to weighted value for each protein (navy, down-represented; yellow, up-represented). **B. *S. aureus* anti-FASII adaptation confers increased H_2O_2 resistance.** USA300 non-treated (NT, orange bar) and AFN-1252-adapted overnight cultures (green bar) were challenged with 0.5 mM H_2O_2 for 5 h, and CFUs were determined. **, p< 0.01. **C. Priming *S. aureus* with H_2O_2 accelerates anti-FASII adaptation and requires PerR. Upper:** USA300 (WT) and *perR* (SAUSA300_1842) mutant SerFA cultures were grown overnight without or with 0.5 mM H_2O_2. Cultures were diluted (OD_{600} = 0.1) in SerFA without or with 0.5 µg/ml AFN-1252, and growth was monitored. Results are shown for biological triplicates. H_2O_2 –primed samples, without or with AFN addition at T0 are as indicated. **Lower:** FA profiles of indicated strains harvested after 6 h anti-FASII treatment (arrow in 'C'). In green, FA profile of fully adapted H_2O_2-pretreated cultures at 10 h, shown here for *perR* and non-distinguishable from WT. 1, 2, and 3, eFAs present in SerFA medium (respectively C14, C16, and C18:1). At left of each profile, proportion of incorporated eFAs (%) are the average of two independent measurements (<3% difference between replicates).

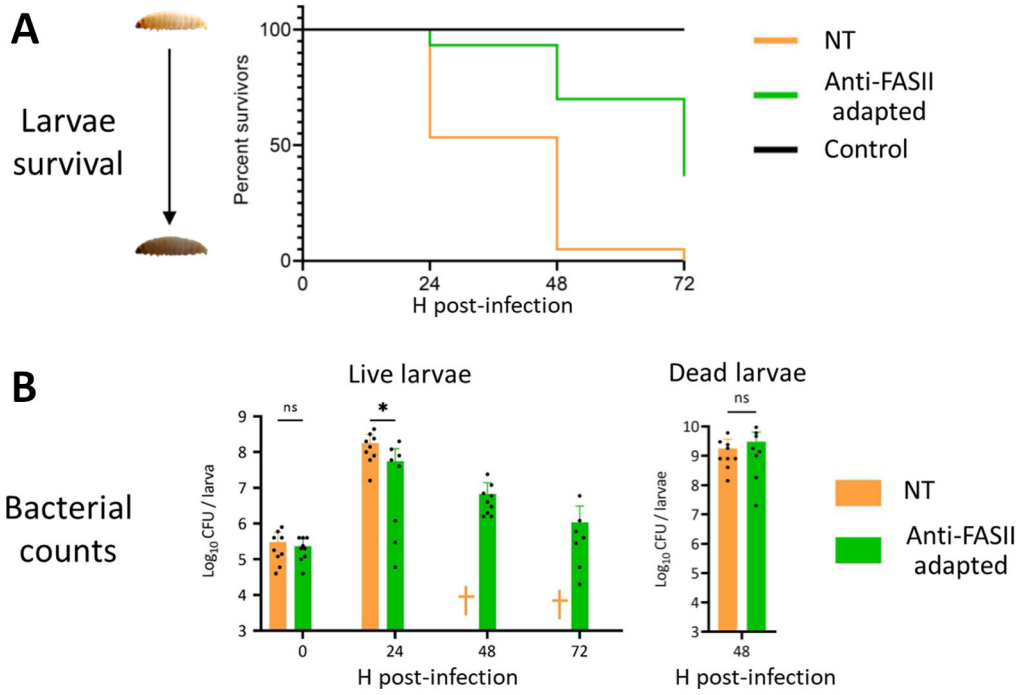

Fig 5. Comparison of untreated and anti-FASII-treated *S. aureus* in a *G. mellonella* infection model. Insects were injected with 10^6 CFU *S. aureus* USA300 that were either non-treated (NT) or preadapted to anti-FASII (anti-FASII adapted) (see Materials and Methods). **A. Insect mortality in NT and anti-FASII-adapted *S. aureus*.** Data was analyzed using Kaplan-Meier with pooled values of biologically independent triplicates (60 insects per condition). Results excluding PBS controls (insects injected with equivalent volumes of PBS, black line) were analyzed by Mantel-Cox, and showed a significance value of $p < 0.0001$. **B. Bacterial CFUs in surviving insects.** Insects were infected as in '**A**'. †, no surviving insects. **C. Bacterial CFUs in dead infected insects at 48 h.** '**B**' and '**C**' analyses were done using the non-parametric Mann Whitney test (Graphpad prism software). *, $p = 0.02$; ns, non-significant.

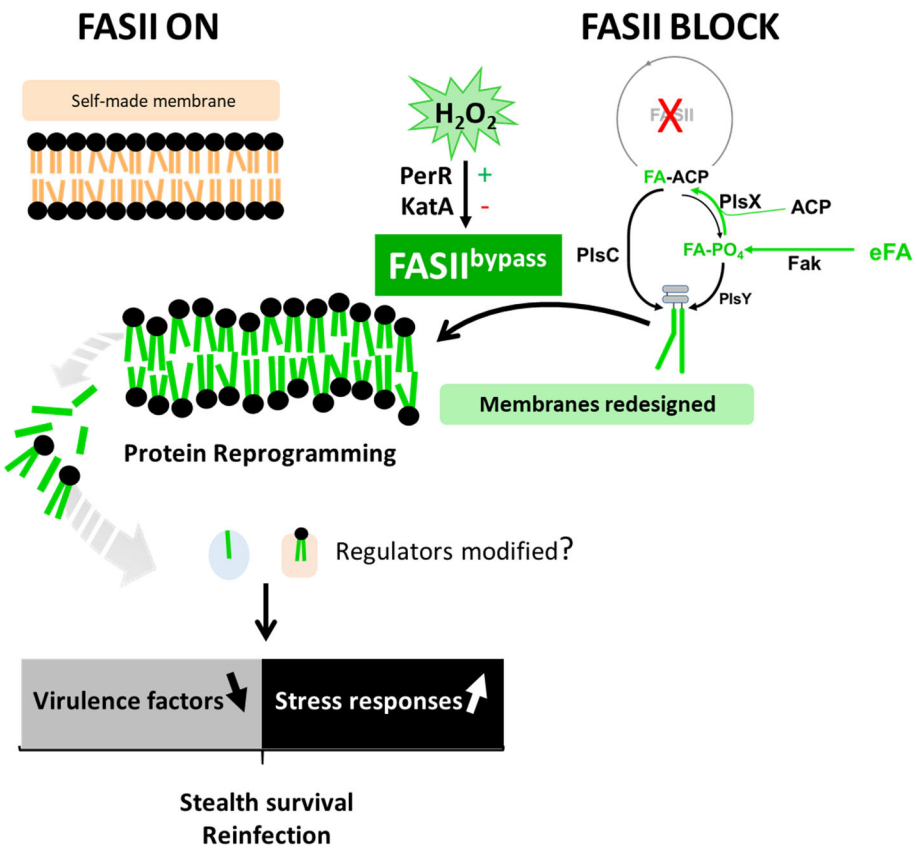

Fig 6. Summary model of anti-FASII adaptation and *S. aureus* fitness. *S. aureus* synthesizes fatty acids (FAs) to produce membrane phospholipids (upper left, FAs in orange). Anti-FASII treatment in SerFA medium promotes FASII bypass, during which exogenous FAs (eFAs, in green) are incorporated and constitute the membrane phospholipid FAs (Kenanian et al., 2019). FASII bypass is accelerated by H_2O_2 priming, which requires PerR, but is lower if KatA is present. Anti-FASII adaptation is accompanied by massive changes in protein expression. Membrane perturbation in the new phospholipid environment is proposed to signal protein reprogramming; as reported, membrane FAs or phospholipids may shed internally and bind to regulatory proteins to modulate their function (Schurig-Briccio et al., 2020, Yeo et al., 2023, Lowden et al., 2010, Huang et al., 2022). Decreased virulence factor production may help bacteria escape host immune surveillance (Tuchscherr et al., 2020). Up-regulation of stress response protein levels confers greater ROS tolerance, and could facilitate survival during infection (DeCoursey, 2004). Peroxide priming accelerates FA incorporation and anti-FASII adaptation by a novel process. Anti-FASII treatment would favor emergence of *S. aureus* populations that are at least transiently less infectious, but that may persist in the host.